WATERFLOOD STABILITY IN SCAL ANALYSIS

Ø. Eide, M. A. Fernø, S. Nybø and A. Graue
Department of Physics and Technology, University of Bergen, Norway

This paper was prepared for presentation at the International Symposium of the Society of Core Analysts held in Avignon, France, 8-11 September, 2014

ABSTRACT

Core analysis using reservoir core plugs is a vital tool when evaluating the performance of production methods or to develop new, improved recovery methods. The size of standard core plugs is small compared with the reservoir, and it is therefore important to take scaling effects into account. Specifically, laboratory experiments are more prone to be influenced by capillary forces with capillary end-effects in both the inlet and outlet face as the most well-known. These effects have little or no effect on the reservoir scale. Capillary end-effects affect the recorded water breakthrough, leading to a time gap between when the waterfront reaches the outlet and water production from the core. Another important, and often ignored, effect is whether or not the waterflood is stable. In a stable waterflood the oil recovery at water breakthrough is independent of injection rate, fluid viscosities and length of the sample. This is particularly important to consider in the recent development in high spatial imaging techniques which have reduced the sample size to a few mm, and flow rates are often very low in order to image dynamic displacement.

Waterflood stability was investigated for three rock types with variations in sample length, absolute permeability and wetting preference. Stability may be evaluated from the product of core plug length, water viscosity and injection rate; termed scaling coefficient. A waterflood is considered stable when there is no change in oil breakthrough with increasing scaling coefficient. The experimental results show significant capillary end-effects at the outlet end of the strongly water-wet cores below stable conditions. End-effects resulted in large time gaps between the arrival of the water front at the outlet face and the breakthrough of water from the core plug. With increasing scaling coefficient, capillary forces became negligible and the time delay between arrival of the front and oil breakthrough was reduced. The total oil recovery was not dependent on the scaling coefficient. In near neutral wetting systems, capillary end-effects were significantly reduced, however, the oil recovery at water breakthrough increased with increasing scaling coefficient until it reached a limiting value at stable conditions. The results show that the scaling coefficient required to achieve waterflood stability will depend on the absolute permeability of the rock, the rock type and the wetting preference.

INTRODUCTION

Experimental results from core analysis are important to building a good model of the reservoir, which in turn determines the production potential and the production strategy. Core analysis is also important when developing new production methods and evaluating existing methods. Because the cores are generally small in comparison with reservoirs it is important to take the scaling effects of the experiments into account. This means that laboratory experiments are more subject to certain forces than full-scale reservoirs, especially capillary end-effects and instabilities in the flow front.

Neglecting capillary end-effects in laboratory waterfloods can lead to erroneous production data, especially for cores with a strong wetting preference. Another important effect which must be taken into consideration is whether or not the flow front is stable. In this context a stable waterflood is characterized by the oil recovery at water breakthrough being independent of changes in flow rate, fluid viscosities and length of the sample. All oil reservoirs can be seen as stable due to their size, however, instabilities in laboratory core floods needs to be avoided in order to simulate field conditions. In laboratory waterfloods it is necessary to use high rates, long cores or high displacing fluid viscosity to achieve stable conditions [17], while at the same time ensure that the applied flow rate does not lead to instabilities in a system where the mobility ratio is high [16].

Waterflood stability has been investigated by several researchers, including [12, 13, 16-19, 22]. Most of this work focuses on the instability of fingering at high flow rates and high mobility ratio. We report an experimental study on standard sized core samples, which demonstrate how instabilities are present in laboratory waterfloods at low flow rates and favorable mobility ratio, and how the capillary end-effects disturb the flow at strongly wetting conditions.

Theoretical Background

Simplified mathematical development of the flooding equations when assuming two incompressible and immiscible fluids injected with constant rate leads to:

$$f\frac{\partial S_w}{\partial t} + V\frac{dF}{dS_w}\cdot\frac{\partial S_w}{\partial x} - \frac{k}{c\mu_w}\cdot\frac{\partial}{\partial x}\left[K_o\cdot F\cdot\frac{dP_c}{dS_w}\cdot\frac{\partial S_w}{\partial x}\right] = 0 \quad (1)$$

where $S_w$is the water saturation, t is time, F is a function of relative permeability and viscosity ratio, x is length, V is injection rate, μ_w is viscosity of water, $K_o$is relative permeability for oil and P_c is capillary pressure. By simplification and substitution Eq. (1) can be developed into:

$$\frac{\partial S_w}{\partial T} + \frac{dF}{dS_w}\cdot\frac{\partial S_w}{\partial X} - \frac{k}{c}\cdot\frac{1}{LV\mu_w}\cdot\frac{\partial}{\partial X}\left[K_o\cdot F\cdot\frac{dP_c}{dS_w}\cdot\frac{\partial S_w}{\partial X}\right] = 0 \quad (2)$$

where X is dimensionless length, T is dimensionless time and L is the total length of the medium.

From Eq. (2) Rapoport and Leas [17] introduced a scaling factor that was the product of length, injection rate and water viscosity (given as length in cm, injection rate as flow rate per unit cross sectional area in cm/min and viscosity as cP). For a standard sized core plug with a radius of 2 cm, a length of 8 cm, porosity 20%, an injection rate of 2 ml/h and water viscosity of 1 cP this gives a scaling coefficient of 0.025 $\mathrm{cm}^2\cdot\mathrm{cp/min}$ Eq. (2) demonstrates that when the scaling coefficient is small, the second order term, containing the capillary pressure, will dominate. This implies that influence of capillary forces during a viscous displacement is highly dependent on the scaling coefficient. Including the absolute permeability in the scaling coefficient implies that the threshold for reaching a stable flood, i.e. where the influence of the capillary forces may be ignored, will be higher in a medium with higher permeability. Because the contact angle, and thus the wettability of the sample, is a factor in the capillary pressure function, a dependency on wettability is also expected in waterfloods. Most oil fields can be considered stable due to their size and length; however, that is not the case for experiments at laboratory scale.

Peters and Flock [16] developed a different instability number:

$$I_{sc} = \frac{(M-1)(v-v_c)\mu_w D^2}{C^* \sigma k_{wor}} \quad (3)$$

Where I_{sc} is the instability number, M is the mobility ratio, v is constant superficial velocity, v_c is characteristic velocity, μ_w is water viscosity, D is diameter, C^* is wettability number, σ is interfacial tension and k_{wor} is effective permeability to water at residual oil saturation.

They found that with an instability number lower than 13.56 the flood was stable, and unstable at higher instability numbers. In this work we have used the instability number from Eq. (2) and found instabilities which correlate to a lower instability number than 13.56 from Eq. (3).

Nuclear Tracer Imaging (NTI)

Nuclear techniques that use gamma rays are far less sensitive to the effects of the pressure vessel surrounding the core than other imaging techniques, and nuclear isotopes in the aqueous phase provide explicit fluid saturation values. The radiation intensity is directly proportional to the fluid saturation, and is detected with a moveable gamma detector outside the pressurized core holder. A 1D fluid saturation profile can be obtained by measuring along the core. The water saturation at a location, "*i"* in the core may be calculated by:

$$S_{iw} = \frac{a_i}{a_{i\,norm}} \quad (4)$$

where a_i is the intensity (disintegration per second) in location i and $a_{i\ norm}$ is the intensity during the normalization scan, i.e. when the core is fully saturated with water. Intensities at each location are corrected for background radiation. The uncertainty of these parameters is the inverse ratio of the square root of the number of counts detected, i.e. uncertainty is decreasing with increasing number of counts detected, expressed by :

$$\Delta a = \frac{1}{\sqrt{N}} \quad (5)$$

where Δa is the uncertainty of disintegrations detected, and N is the number of counts. The uncertainty of the calculated water saturation at a point, "*i"* along the core may be found by solving:

$$\Delta S_{iw} = \sqrt{\left(\frac{\Delta a_i}{a_{inorm}}\right)^2 + \left(\frac{a_i}{a^2{}_{inorn}} \Delta a_{inorm}\right)^2} \quad (6)$$

where ΔS_{iw} is the uncertainty in the calculated water saturation at location i, Δa_i is the uncertainty of the disintegrations detected at location i and Δa_{inorm} is the uncertainty in intensity during the normalization profile. Under typical experimental conditions, Δa_i is in the order of 2%, while Δa_{inorm} is generally smaller (about 1%) due to higher N, see eq. (5). A more detailed description of the NTI technique can be found in [6, 8].

EXPERIMENTAL PROCEDURES

Core preparation

Core plugs were cut from larger slabs of rocks obtained at three outcrops. The core plugs were dried at 90°C for at least 3 days before they were vacuum saturated with brine. After saturation, standard core analysis was performed and the results are summarized in Table 1.

Rørdal chalk

The rock formation was of Maastrichtian age and consists mainly of coccolith deposits. The composition is calcite (99%) with some quartz (1%). Porosity and permeability ranges from 45-47% and 3-8 mD, respectively. Further geological characterization may be found in [3, 9, 14, 21].

Edwards Limestone

The rock material is composed of calcite minerals with pore space consisting mainly of moldic pores (derived from dissolution of fossils) and interparticle porosity. The original interparticle porosity was reduced significantly by recrystallization of calcite. BET surface area ranges from 0.2-0.4m^2/g. Porosities in core plugs drilled from the same block ranges from 0.18-0.26, whereas the absolute permeability to brine ranges from 5-20 mD. More details may be found in [4, 20, 23].

Bentheim Sandstone

The rock material is composed of almost pure quartz (95%) with some kaolinite and orthoclase [11]. Porosity and permeability ranges from 22-25% and 1-2 D, respectively.

Fluids

Brine compositions and fluid properties are listed in Table 2.

Wettability alteration

To change the wettability to near neutral-wet conditions, core samples P4 and P5 were aged using dynamic ageing [1, 5, 7]. The cores were drained with crude oil at constant pressure drop of 1.5 bar/cm. After primary drainage, crude oil was injected at constant injection rate at elevated temperature. Core sample P5 was aged for 10 days, and P4 for 5 days, with the direction of flow being reversed after half the aging time. The established wettability preference after aging was measured by the Amott-Harvey wettability test. The cores not treated with crude oil are assumed to be strongly water-wet, based on previous experiments [10] and measurements on sister plugs. Wetting preference for each core is listed in Table 1.

Brine displacement

After standard core analysis, the strongly water-wet cores were flushed with radioactive brine containing the radioactive isotope Na^{22} to do a miscible exchange of fluids. Na^{22} was selected because it is an isotope of sodium which is already present in the brine [2]. In the aged core sample water was injected at constant pressure to reach irreducible water saturation before the miscible displacement. The emitted γ-rays from the radioactive brine were detected by a movable Germanium detector mounted on rails and controlled by a step motor. This provided a 1D profile of γ-ray intensity, which is proportional to the saturation. A more detailed description of the NTI technique may be found elsewhere [6, 8].

Waterflooding

Before each experiment the core samples were oil flooded to irreducible water saturation (S_{wi}) before being waterflooded at a constant injection rate. After each waterflood, the core sample was

oil flooded back to S_{wi} and waterflooded again with a different constant injection rate, corresponding to a different scaling coefficient. Special care was taken to ensure that the irreducible water saturation was identical before each waterflood. The maximum water injection rate was determined by the differential pressure to ensure the integrity of the cores, meaning that the maximum injection rate was higher in the sandstone compared to the chalk. Water saturation at water breakthrough was recorded by monitoring the produced fluids with a fraction collector, or visual inspection using a camera. The water arrival at the outlet end of the core was identified using the *in-situ* data from NTI.

RESULTS AND DISCUSSION

The first experiments were performed on strongly water-wet cores to replicate the results by [15] and [13]. The second part of this work seeks to investigate the effect of wettability on outlet capillary end-effects as well as waterflood stability. Note that these experiments were performed at a low oil-to-water viscosity ratio, which means viscous fingering is not expected to be significant. Note that all production curves are showing oil recovery as fraction of total pore volume, this is to directly compare to the work of Kyte and Rapoport [13].

Water-wet limestone

Figure 1 shows oil production from material balance at different injection rates in strongly water-wet limestone EDW2. Water breaks through at the outlet after about 0.35 PVs injected, with total oil recovery of 0.33 of total PV. The core sample exhibited strongly water-wet characteristics, with no transient production of oil and water. At high injection rates the production of oil at water breakthrough rises, this is most likely caused by capillary de-saturation. The water front arrivals are indicated as points on the recovery curve.

Water-wet chalk

Figure 2 shows the oil recovery as fraction of pore volume vs. pore volumes injected in strongly water-wet chalk core P6L using increasing water injection rates. Water was produced after 0.40 PVs injected and the total oil recovery was 0.40 of total PV with no transient production of water and oil. Because of the brittle nature of the chalk, capillary de-saturation was not reached in this sample. The results demonstrate that the influence of the capillary end-effects was reduced as the injection rates, and the scaling coefficient, increased. That is because at low injection rates the water arrival at the outlet of the core sample was up to 0.2 PVs before water was produced. Without capillary end-effects, we would expect transient production after water arrival at the outlet of the core, especially at lower injection rates, i.e. at lower scaling coefficients.

Water-wet sandstone

Figure 3 shows the oil recovery vs. pore volumes injected in strongly water-wet sandstone core SN1 using increasing water injection rates from 3-3000 ml/h. No additional oil was produced after water breakthrough for all injection rates. At low injection rates water breakthrough occurred after 0.30 PVs injected, and total oil recovery was 0.29 of total PV. At higher injection rate the oil recovery at water breakthrough increased slightly. Capillary de-saturation was reached at a slightly higher scaling coefficient than in core plug EDW2, as demonstrated in Figure 4.

Figure 4 shows a summary from all strongly water-wet core plugs P6L (blue), EDW2 (black) and SN2 (red). Water arrival (dashed) and water breakthrough (drawn) is plotted on the y-axis with the scaling coefficient on a logarithmic x-axis. Every data point represents one waterflood. The results in Figure 4 correlates with earlier results from [13], and demonstrates that the scaling

coefficient required to generate a stable flood and reduce capillary end-effects, i.e. eliminate the gap between water arrival and water breakthrough, were different for the three cores. The required scaling coefficient systematically increased with increasing absolute permeability: for chalk (K=4.6 mD) a scaling coefficient above 0.6 was needed; for limestone (K=11.8 mD) a scaling coefficient above 0.8; for sandstone (K=1000mD) a scaling coefficient above 1.5 was required. With increasing scaling coefficient the injection rates increased significantely, increasing the capillary de-saturation. Results suggest that capillary desaturation may occur at a lower scaling coefficient in limestone (EDW2) compared with sandstone (SN2), probably due to the lower permeability of limestone with more pronounced viscous forces. Above this scaling factor the waterflood seems to be stable until the scaling coefficient exceeds 10 and capillary de-saturation occurs. A scaling coefficient of 10 correlates to an injection rate of nearly 800 ml/hr, or 165 ft/day, which is far higher than any field injection rate. That means that capillary de-saturation will not be a problem in most laboratory waterfloods, unlike capillary end-effects.

Near neutral-wet chalk cores

The change in the required scaling coefficient for stable waterfloods at less water-wet wettability conditions was investigated using aged chalk cores. Figure 5 shows the time lag (in fraction pore volumes injected) between the waterfront arrival at the outlet (dashed) and the observed water breakthrough from the outlet (drawn) as a function of scaling coefficient for chalk cores of different wettability. Each data point in Figure 5 represents one waterflooding experiment. Strongly water-wet core P6L (black) demonstrated a time lag between arrival and water production up to a scaling coefficient of 0.6. The corresponding results for less water-wet conditions demonstrate that no time lag was observed for core plug P5 (green), whereas a small difference was observed for core plug P4 (blue). The results from Figure 5 also indicate that having a near neutral-wet core would lower the scaling coefficient needed for a stable flood. This can be seen from P5 as it seems to stabilize somewhat earlier than P6L. However, it is not very visible in P4, which means that more experiments in cores with different wettability is needed to determine the effect.

CONCLUSIONS

The experimental results clearly show that scaling and stabilization properties should be taken into account when reporting oil recovery vs pore volumes injected based on laboratory waterfloods. It demonstrates how capillary end-effects are prominent in strongly water-wet samples, and less so in near neutral-wet samples. It also shows that it is necessary to take the permeability of the sample into consideration when trying to establish stable conditions. A higher scaling coefficient was needed for a stable flood at higher permeability. The experiments also show that while the capillary end-effects were less significant at near neutral-wet conditions, the flood still exhibited stabilization properties. The scaling coefficient needed for a stable waterflood in the near neutral-wet samples appears to be slightly lower than in the corresponding strongly water-wet samples, however this effect was not visible in all the samples studied.

ACKNOWLEDGMENTS

The authors are indebted to Riley Needham of ConocoPhillips for initiating the work and assisting in the interpretation of the results. The authors would also like to thank the Norwegian Research Council for financial support. Statoil, BP and ConocoPhillips are also thanked for their financial contributions.

REFERENCES

1. Aspenes, E., A. Graue and J. Ramsdal, *In situ wettability distribution and wetting stability in outcrop chalk aged in crude oil.* Journal of Petroleum Science and Engineering, 2003. **39**(3-4): p. 337-350.
2. Bailey, N.A., P.R. Rowland and D.P. Robinson. *Nuclear Measurements of Fluid Saturation in EOR Flood Experiments*. in *European Symposium on Enhanced Oil Recovery*. 1981. Bournemouth, UK.
3. Ekdale, A.A. and R.G. Bromley, *Trace Fossils and Ichnofabric in the Kjølby Gaard Marl, Uppermost Creataceous, Denmark.* Bull Geol. Soc. Denmark, 1993. **31**: p. 107-119.
4. Fernø, M.A., *An Experimental Investigation of Rock Characteristics and Waterflood Oil Recovery in Outcrop Carbonate Rock at Various Wettability Conditions*, in *Dept. of Physics and Technology*2005, University of Bergen: Bergen, Norway.
5. Fernø, M.A., M. Torsvik, S. Haugland and A. Graue, *Dynamic Laboratory Wettability Alteration.* Energy & Fuels, 2010. **24**(7): p. 3950-3958.
6. Graue, A., *Imaging the Effect of Capillary Heterogeneites on Local Saturation Development in Long-Core Floods.* SPEDC, 1994. **9**(1).
7. Graue, A., E. Aspenes, T. Bogno, R.W. Moe and J. Ramsdal, *Alteration of wettability and wettability heterogeneity.* Journal of Petroleum Science and Engineering, 2002. **33**(1-3): p. 3-17.
8. Graue, A., K. Kolltveit, J.R. Lien and A. Skauge, *Imaging Fluid Saturation Development in Long-Core Flood Displacements.* SPE Form. Eval., 1990. **5**(4): p. 406-412.
9. Hjuler, M.L., *Diagenesis of Upper Cretaceous onshore and offshore chalk from the North Sea area*, in *Institute of Environment & Resources*2007, Technical University of Denmark: Copenhagen, Denmark.
10. Johannesen, B., Else, *Wettability Determined by NMR and its Impacts on Oil Recovery in Chalk*, in *Institute for Physics and Technology*2008, University of Bergen: Bergen. p. 150.
11. Klein, E. and T. Reuschle, *A model for the mechanical behaviour of Bentheim sandstone in the brittle regime.* Pure and Applied Geophysics, 2003. **160**(5-6): p. 833-849.
12. Krause, M.H., *Modeling and Investigation of the Influence of Capillary Heterogeneity on Relative Permeability*2012.
13. Kyte, J.R. and L.A. Rapoport, *Linear Waterflood Behavior and End Effects in Water-Wet Porous Media.* Transactions of the American Institute of Mining and Metallurgical Engineers, 1958. **213**(12): p. 423-426.
14. Odling, N.E., P. Gillespie, B. Bourgine, C. Castaing, J.P. Chiles, N.P. Christensen, E. Fillion, A. Genter, C. Olsen, L. Thrane, R. Trice, E. Aarseth, J.J. Walsh and J. Watterson, *Variations in fracture system geometry and their implications for fluid flow in fractures hydrocarbon reservoirs.* Petroleum Geoscience, 1999. **5**(4): p. 373-384.
15. Perkins, F.M., *An Investigation of the Role of Capillary Forces in Laboratory Water Floods.* Transactions of the American Institute of Mining and Metallurgical Engineers, 1957. **210**(12): p. 409-411.
16. Peters, E.J. and D.L. Flock, *The Onset of Instability During Two-Phase Immiscible Displacement in Porous Media.* Society of Petroleum Engineers Journal, 1981. **21**(2): p. 249-258.
17. Rapoport, L.A. and W.J. Leas, *Properties of Linear Waterfloods.* Transactions of the American Institute of Mining and Metallurgical Engineers, 1953. **198**: p. 139-148.
18. Riaz, A., G.-Q. Tang, H.A. Tchelepi and A.R. Kovscek, *Forced imbibition in natural porous media: Comparison between experiments and continuum models.* Physical Review E, 2007. **75**(3): p. 036305.
19. Richardson, J.G. and F.M.P. Jr., *A Laboratory Investigation of the Effect of Rate on Recovery of Oil by Water Flooding*1957.
20. Seth, S. and N.R. Morrow, *Efficiency of the Conversion of Work of Drainage to Surface Energy for Sandstone and Carbonate.* SPE Reservoir Eval. & Eng., 2007. **10**(4): p. 338-347.

21. Strand, S., M.L. Hjuler, R. Torsvik, J.I. Pedersen, M.V. Madland and T. Austad, *Wettability of chalk: impact of silica, clay content and mechanical properties.* Petroleum Geoscience, 2007. **13**(1): p. 69-80.
22. Tang, G.Q. and A.R. Kovscek, *High Resolution Imaging of Unstable, Forced Imbibition in Berea Sandstone.* Transport in Porous Media, 2011. **86**(2): p. 617-634.
23. Tipura, L., *Wettability Characterization by NMR T2 Measurements in Edwards Limestone*, in *Dept. of Physics and Technology*2008, University of Bergen: Bergen, Norway.

Table 1: Core properties

Core ID	P4	P5	P6L	EDW2	SN1
Type	Rørdal chalk	Rørdal chalk	Rørdal chalk	Edwards limestone	Bentheim sandstone
Length [cm]	8.00	7.97	13.92	14.94	15.22
Radius [cm]	2.54	2.53	2.77	2.40	2.59
Porosity [%]	46	48	46	21	25
Permeability [mD]	6.2	14.0	4.6	11.8	N/A
Amott index for water	0.1	0*	1*	1*	1*

*Not experimentally measured, measured on sister plugs

Table 2: Fluid properties

Name	Description / Contents	Density [g/cm^3]	Viscosity 20^0 C [cP]
Brine	Distilled water 5 Wt-% NaCl 0.0005 Wt-% NaN_3	1.03	1.07
Filtered mineral oil	Mineral oil	0.74	1.47

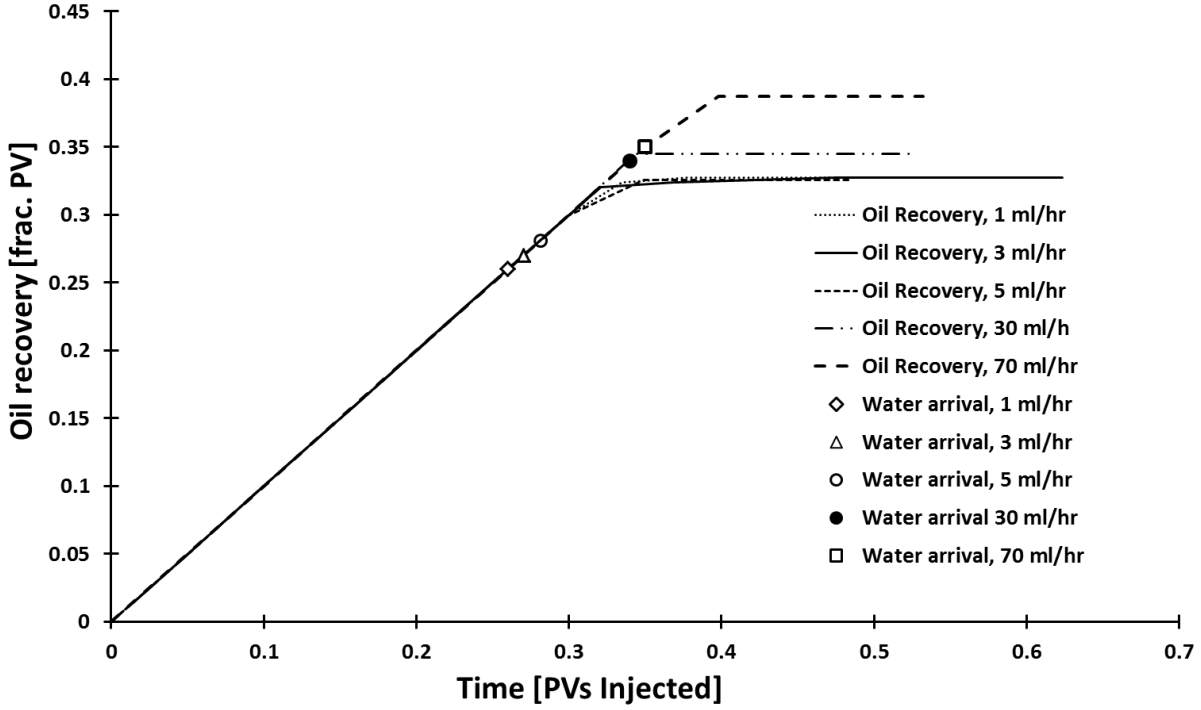

Figure 1: Oil recovery vs. pore volumes injected for limestone core plug EDW2 using different injection rates from 1-70ml/h. The arrival of the waterfront at the outlet is indicated for each rate.

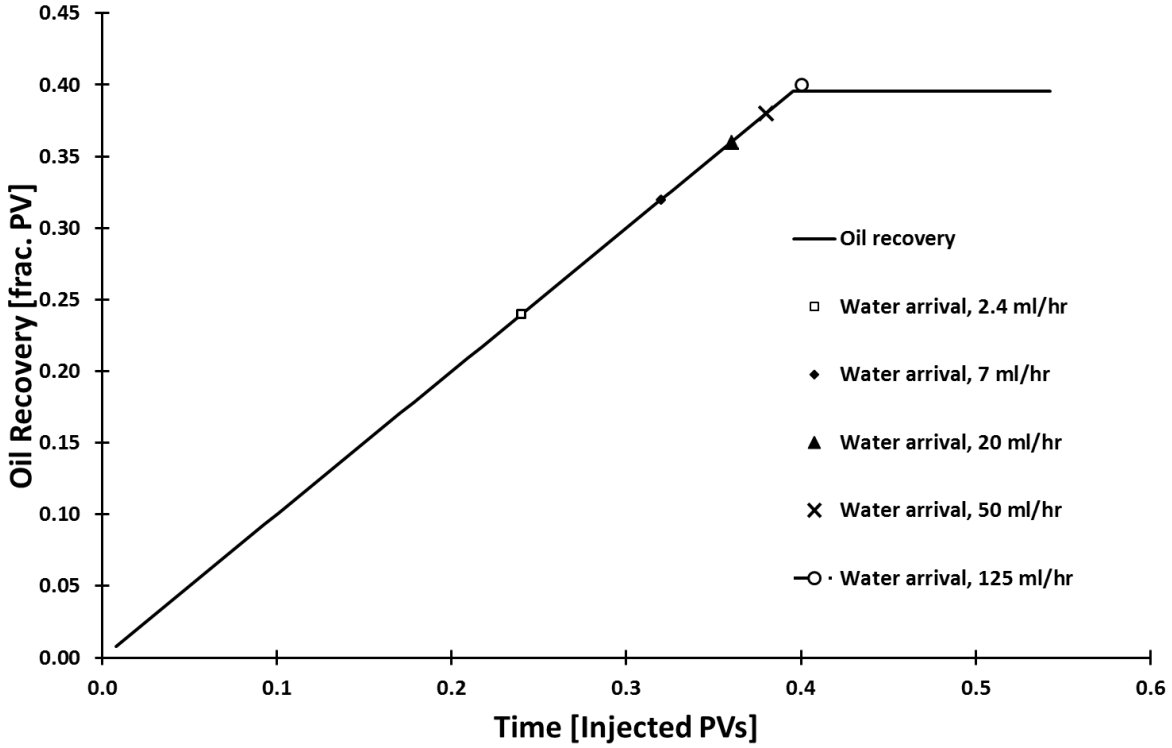

Figure 2: Oil recovery vs. pore volumes injected for chalk core plug P6L using different injection rates from 2.4-125ml/h. The arrival of the waterfront at the outlet is indicated for each rate.

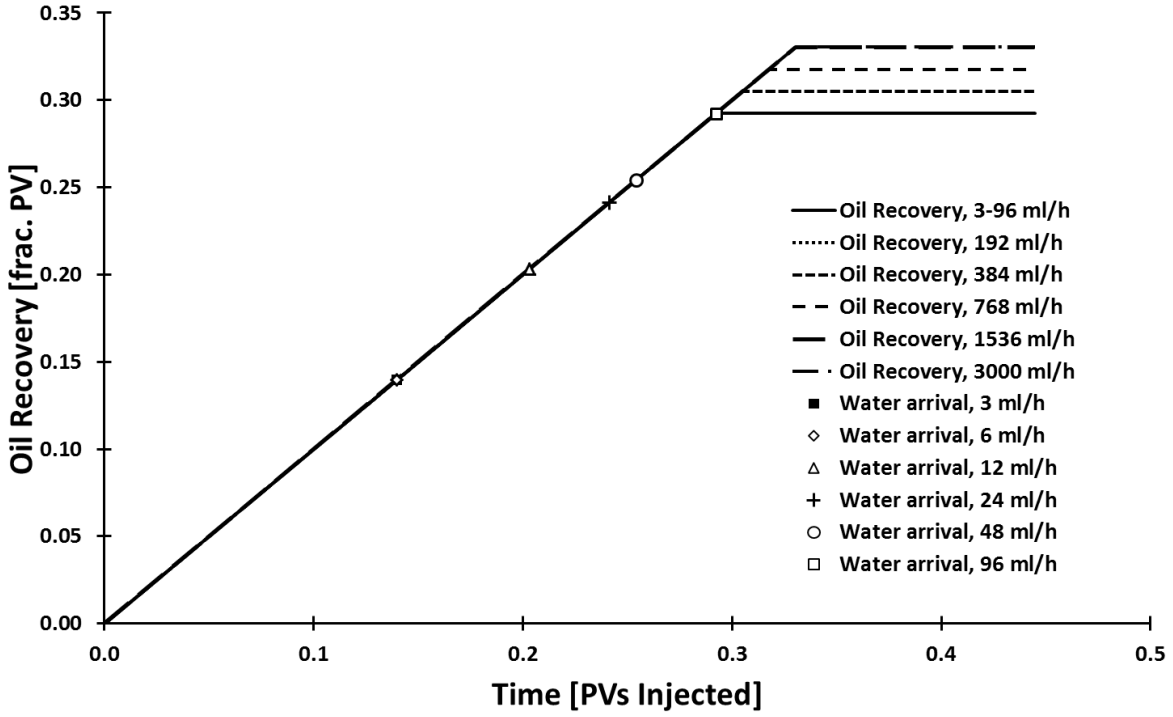

Figure 3: Oil recovery vs. pore volumes injected for sandstone core plug SN1using different injection rates from 3-3000ml/h. The arrival of the waterfront at the outlet is indicated for each rate.

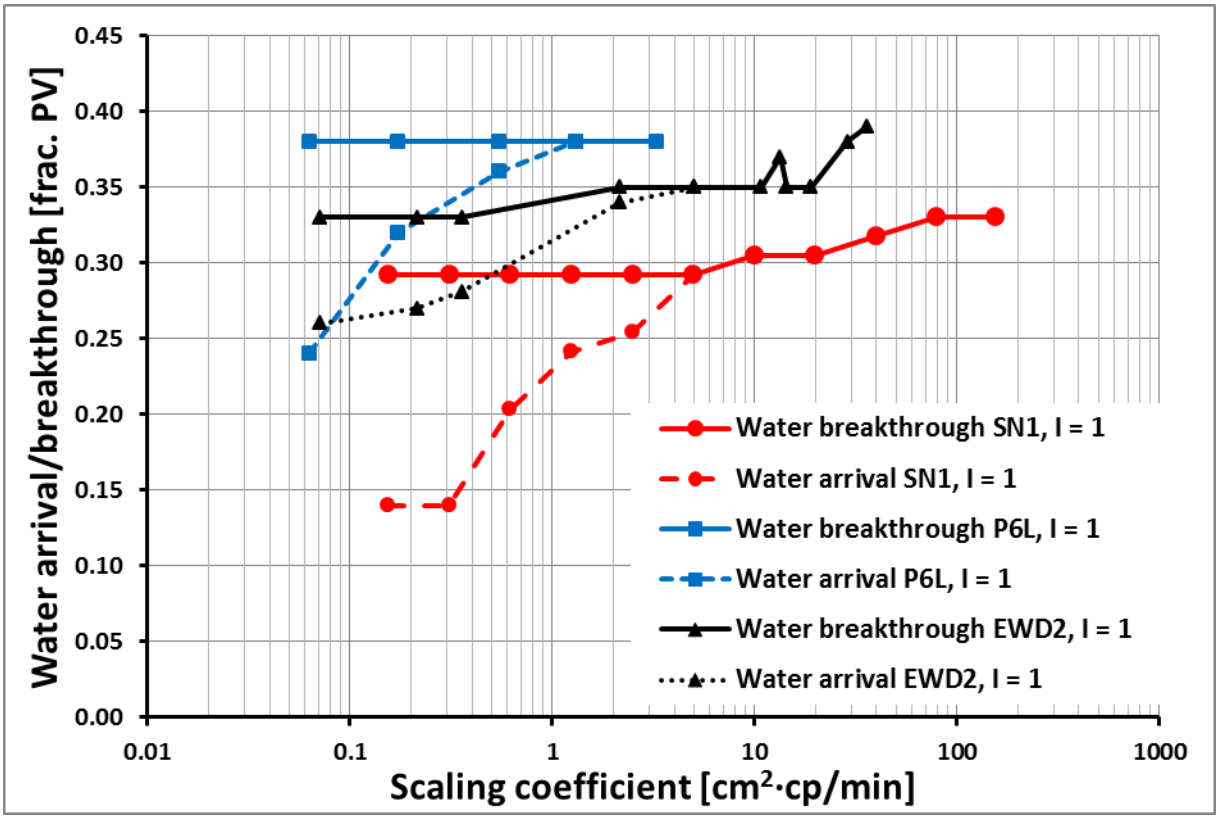

Figure 4: Correlation of waterflood test data, strongly water-wet cores, P6L, SN1 and EDW2 at different scaling coefficients

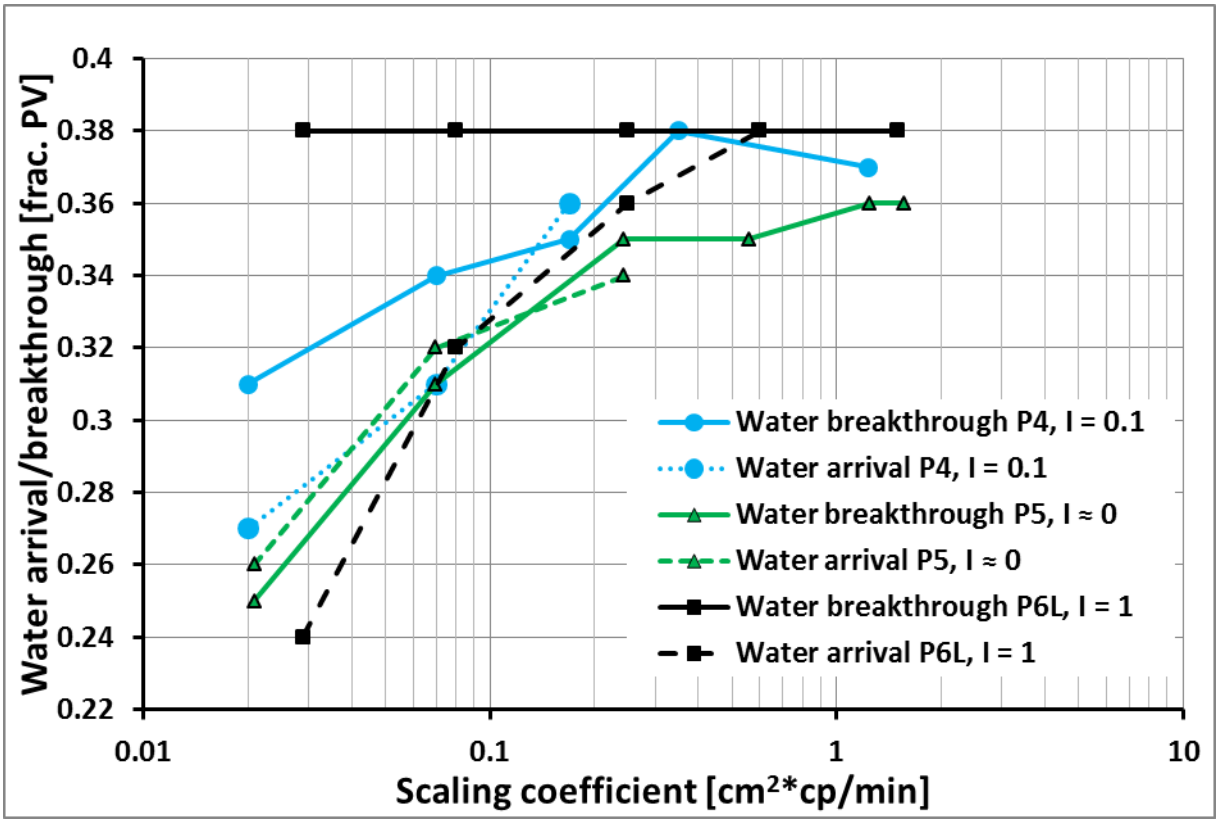

Figure 5: Correlation of waterflood test data, strongly water-wet core P6L and near neutral wet cores P4 and P5 at different scaling coefficients.